

Carbamoyl Triazoles, Known Serine Protease Inhibitors, Are a Potent New Class of Antimalarials

Matthew McConville,[†] Jorge Fernández,[†] Íñigo Angulo-Barturen,[†] Noemi Bahamontes-Rosa,[†] Lluís Ballell-Pages,[†] Pablo Castañeda,[†] Cristina de Cózar,[†] Benigno Crespo,[†] Laura Guijarro,[†] María Belén Jiménez-Díaz,[†] María S. Martínez-Martínez,[†] Jaime de Mercado,[†] Ángel Santos-Villarejo,[†] Laura M. Sanz,[†] Micol Frigerio,[‡] Gina Washbourn,[‡] Stephen A. Ward,[§] Gemma L. Nixon,[‡] Giancarlo A. Biagini,[§] Neil G. Berry,[‡] Michael J. Blackman,^{||} Félix Calderón,^{*,†,||} and Paul M. O'Neill^{*,‡}

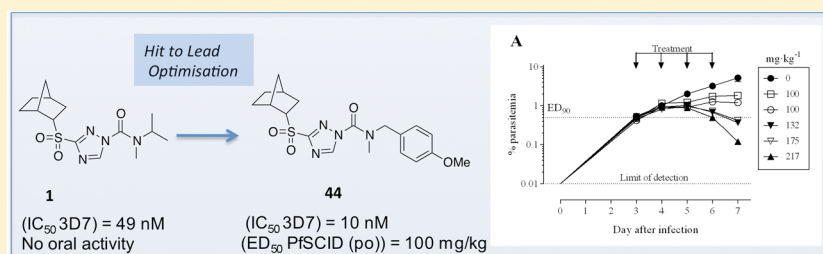
[†]Tres Cantos Medicines Development Campus, DDW, GlaxoSmithKline, Severo Ochoa 2, 28760 Tres Cantos, Spain

[‡]Department of Chemistry, University of Liverpool, Liverpool L69 7ZD, United Kingdom

[§]Liverpool School of Tropical Medicine, Pembroke Place, Liverpool L3 5QA, United Kingdom

^{||}Division of Parasitology, MRC National Institute for Medical Research, Mill Hill, London NW7 1AA, United Kingdom

S Supporting Information



ABSTRACT: Screening of the GSK corporate collection, some 1.9 million compounds, against *Plasmodium falciparum* (Pf), revealed almost 14000 active hits that are now known as the Tres Cantos Antimalarial Set (TCAMS). Followup work by Calderon et al. clustered and computationally filtered the TCAMS through a variety of criteria and reported 47 series containing a total of 522 compounds. From this enhanced set, we identified the carbamoyl triazole TCMDC-134379 (1), a known serine protease inhibitor, as an excellent starting point for SAR profiling. Lead optimization of 1 led to several molecules with improved antimalarial potency, metabolic stabilities in mouse and human liver microsomes, along with acceptable cytotoxicity profiles. Analogue 44 displayed potent in vitro activity (IC₅₀ = 10 nM) and oral activity in a SCID mouse model of Pf infection with an ED₅₀ of 100 and ED₉₀ of between 100 and 150 mg kg⁻¹, respectively. The results presented encourage further investigations to identify the target of these highly active compounds.

INTRODUCTION

Malaria, the disease caused by parasites of the *Plasmodium* genus, results in approximately 0.7 million deaths per annum and is responsible for some 660 million clinical cases worldwide.¹ Malaria affects some of the most vulnerable people in the world, particularly children and pregnant women in resource-poor regions such as sub-Saharan Africa and South East Asia. The current frontline treatments for *falciparum* malaria, the most deadly species, are artemisinin based combination therapies.² These consist of the coadministration of a highly efficacious but rapidly cleared artemisinin derivative³ (dihydroartemisinin, artemether, or artesunate) with another, longer acting secondary agent, typically lumefantrine or piperazine.² A current area of global concern in malaria is the emergence of resistance to antimalarial drugs, including the artemisinins, which renders them ineffective.^{4–8} Recent reports have confirmed that parasites with reduced susceptibility to artemisinins, reflected in a slow parasite clearance rate, have

been discovered in Southeast Asia.^{9–12} The issue of resistance coupled with the demand of a newly accepted set of antimalarial target product profiles¹³ has prompted the search for antimalarials with novel mechanisms of action that can be deployed for treatment of all malaria species for prophylaxis and transmission blocking.

Screening of the GSK corporate collection, some 1.9 million compounds, against *Plasmodium falciparum* (Pf), revealed almost 14000 active hits that are now known as the Tres Cantos Antimalarial Set (TCAMS).¹⁴ Further work by Calderon et al. filtered the TCAMS through a variety of criteria (activity, physicochemical properties, similarity indices, molecular weight, functional groups, scaffold novelty, etc.) and reported 47 series containing a total of 522 compounds.¹⁵ From these compounds, we chose the carbamoyl triazole TCMDC-

Received: March 18, 2015

134379 (**1**, Figure 1) as a starting point for further development. Carbamoyl triazoles have been extensively

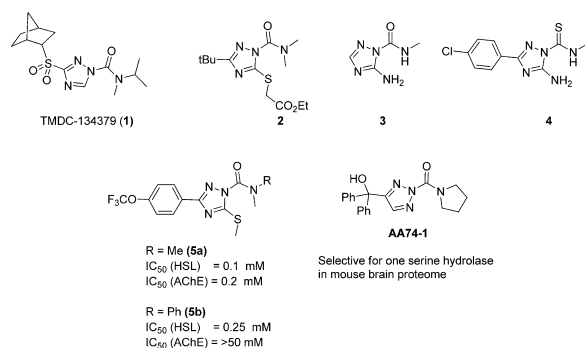


Figure 1. Biologically active carbamoyl triazoles.

reported as herbicides,¹⁶ fungicides,¹⁷ and insecticides,¹⁸ particularly in the patent literature. Triazamate (Aphistar, **2**) is a commercial insecticide used in the control of aphids on various crops and kills insects by inhibition of acetylcholine esterase (AChE). Carbamoyl triazoles such as **3** and the related thiocarbamoyl triazole **4** were shown to be effective at reducing sephadex-induced eosinophilia in rats when administered both po and ip.¹⁹ **4** was shown to have low toxicity (LD_{50} > 2000 mg kg^{-1}) in mice. Jacobsen et al. reported carbamoyl triazoles were potent inhibitors of hormone sensitive lipase (HSL), an esterase responsible for regulation of fatty acid metabolism.²⁰ They found that, although selective over hepatic, lipoprotein, pancreatic, and butyrylcholine esterases, the compounds were still inhibitors of acetylcholine esterase (AChE). Given **5**'s similarity to **2**, this is hardly surprising. However, by exchanging an *N*-Me (**5a**) for *N*-Ph (**5b**), they were able to improve the selectivity for HSL over AChE by more than 2 orders of magnitude, demonstrating that designing in selectivity is possible for these compounds. A pseudoreversible mechanism of inhibition involving acylation of the active site serine is proposed. Cravatt et al. showed that carbamoyl triazoles are remarkably selective for the serine protease class of enzyme.²¹ Furthermore, they were able to demonstrate excellent selectivity for a single serine protease in the mouse brain proteome after synthesizing a series of carbamoyl 1,2,3-triazole analogues. AA74-1 was able to completely and selectively inhibit the serine hydrolase APEH in vivo at ip doses of 0.4 mg kg^{-1} . These studies show the potential of the carbamoyl triazoles to be developed as selective and potent pharmaceutical compounds.

RESULTS AND DISCUSSION

1 was attractive for several reasons. It is highly potent in vitro (IC_{50} = 49 nM) against *Pf*, and it represents a chemical scaffold that is unique to known antimalarial compounds (Table 1). **1** is a potent inhibitor of the serine protease dipeptidyl peptidase IV (DPP-IV) (IC_{50} = 9 nM).²² Serine proteases are a relatively unexplored class of enzyme for antimalarial compounds, so there is potential to exploit novel enzyme targets in this class.^{23–28} The likely mechanism of action is irreversible inhibition by carbamylation of nucleophilic serine residues in the active site. Carbamoyl triazoles are reported to increase glucose tolerance in mice, through DPP-IV inhibition, with oral doses as low as 1 mg kg^{-1} .²² **1** has physicochemical properties favorable for oral drugs (ChromlogD = 4.9, solubility

Table 1. In Vitro and In Vivo Data for Compound **1**

measurement	value
Cl_{int} $mL\ min^{-1}\ g^{-1}$ (m/h) ^a	18.2/1.6
in vitro $t_{1/2}$ min (m/h)	3.8/>30
HSA ^b binding (%)	58
CYP3A 4VG/4VR IC_{50} (μM)	>50/31.6
ChromlogD (PFI) ^c	4.82 (5.8)
Tox ₅₀ HepG2 (μM)	>100
<i>P. berghei</i> , 2 doses, ^d 50 mg kg^{-1}	ED_{50} > 50 mg kg^{-1}

^a(mouse/human). ^bHuman serum albumin. ^cPFI = ChromlogD + no. of aromatic rings. ^dp.o.

(chemoluminescent nitrogen detection kinetic solubility (CLND) \geq 500 μM), passive permeability (PAMPA) >300 nm/s). In vitro pharmacological profiling which involves the screening of **1** against a broad range of human targets (receptors, ion channels, enzymes, and transporters) in order to identify specific molecular interactions that may cause adverse drug interaction in humans revealed no major concerns. Cytotoxicity against HepG2 cells was shown to have IC_{50} > 100 μM . A QPatch assay was negative for hERG inhibition. High clearance in mouse liver microsomes (Cl_{int} = 18.2 $mL\ min^{-1}\ g^{-1}$) demonstrated that metabolic stability was likely to provide an optimization challenge in this series. However, it should be noted that the values in human liver microsomes were significantly lower (Cl_{int} = 1.6 $mL\ min^{-1}\ g^{-1}$). From a medicinal chemistry point of view, the compound was also attractive as it offers several sites for modification with high synthetic tractability.

There was, however, some cause for concern with respect to plasma/blood stability and consequent in vivo efficacy given the instability of the hit compound in both plasma and blood (Figure 2). Addition of protease/esterase inhibitors showed

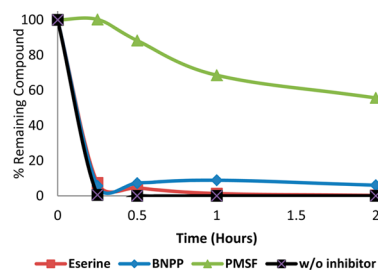


Figure 2. Mouse blood stability assays for **1** with and without various esterase/protease inhibitors.

that PMSF, a known, nonselective serine protease inhibitor, was able to significantly increase the mouse blood stability of the hit compound. This evidence indicates that proteases/esterases are the likely culprits for the instability.

A preliminary evaluation of the in vivo efficacy (p.o. administration) of **1** against a *P. berghei* murine model of malaria infection showed a lack of oral efficacy (ED_{50} > 50 mg kg^{-1}). Given the efficacy of related compounds with respect to glucose tolerance and the high potency of **1** in vitro against *Pf*, this result was surprising. The reason for this discrepancy could be explained by the different sites of action for glucose tolerance and antiparasmodial effects. DPP-IV is responsible for the deactivation of glucagon-like peptide-1 (GLP-1).²⁹ GLP-1 stimulates insulin and inhibits glucagon secretion. It follows that inhibition of DPP-IV increases the level of active GLP-1

and, through the action of GLP-1 on insulin and glucagon, lowers blood glucose (increased glucose tolerance). The interaction of DPP-IV/GLP-1 takes place predominantly on the brush border epithelium of the small intestine.³⁰ As a consequence, orally administered DPP-IV inhibitors do not have to enter the systemic circulation to exert their effect on glucose tolerance. On the other hand, to effectively affect malaria parasites, compounds must pass through the brush border epithelium, into the systemic circulation and finally into erythrocytes where the *Plasmodium* targets are located. Given that **1** is a likely irreversible inhibitor of DPP-IV (and other proteases) and shows low stability in blood, it can be seen that the difference in oral efficacy between plasmodial infection and glucose tolerance is explicable through the differing sites of action. The challenge was, therefore, to moderate the reactivity of the carbamoyl group in such a way that the antiparasmodial activity is retained, plasma/blood stability is increased, and clearance is reduced. This could conceivably be achieved by altering the steric and electronic properties of the carbamoyl group.

Further in vitro assays allowed us to gain more information with regard to the antiparasmodial effects of **1**. The parasite reduction ratio (PRR) assay is used to measure the killing kinetics of compounds against *Plasmodium falciparum*.³¹ Several parameters can be determined from the assay and the killing profile compared to known antimalarial compounds previously reported. The assay is run at $10 \times \text{IC}_{50}$ of the compound to be studied. In vitro PRR represents the decrease in viable parasites by a drug treatment over one life cycle (48 h for *Pf*), and it is a direct measurement of the killing rate of an antimalarial drug. Figure 3 shows that, for **1**, $\log_{10} \text{PRR} = 3.1$, $\text{PCT}_{99.9\%} = 48 \text{ h}$,

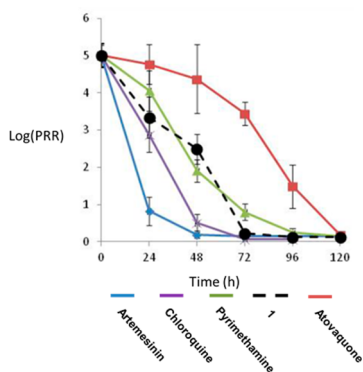


Figure 3. PRR assay of **1** (black) compared to that of artemisinin (blue), atovaquone (red), pyrimethamine (green), and chloroquine (purple).

and there is no lag phase. **1** has a profile between that of previously reported profiles for pyrimethamine and chloroquine³¹ and is classified as a moderate killer.

To determine the SAR, a range of analogues were synthesized and tested in vitro against *Pf*. Three main areas were identified for SAR exploration (Figure 4): (i) The secondary amide substituents of the carbamoyl group, R' and R'' . Various combinations of aryl, alkyl, and benzyl were considered in order to control the steric and electronic properties of the carbonyl group thought to be key to the serine protease inhibiting activity. (ii) The linker group (Y) separating the triazole ring from the varying R groups. Varying between the electron donating sulfide and electron withdrawing sulfone allows dramatic changes in the electronic properties

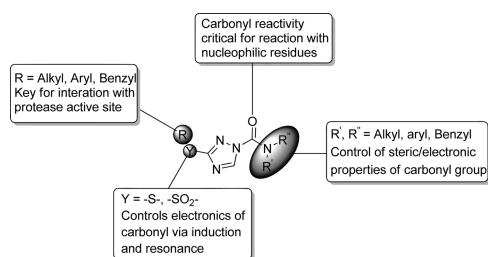
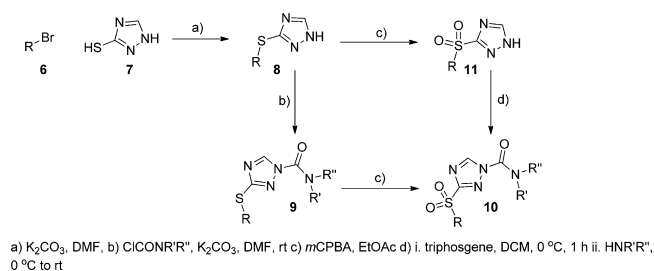


Figure 4. Key SAR features of carbamoyl triazoles.

and, therefore, reactivity of the carbamoyl group. This change is also attractive from a tractability point of view as the sulfones are accessible from the sulfides via simple oxidation. (iii) The R group bonded to linker Y . Although remote from the carbamoyl group and unlikely to influence the reactivity directly, the R group should have profound effects on activity by way of mediating the interaction with protease active sites. The S_1/S_1' sites of proteases play a vital role in substrate recognition/binding, and therefore groups remote to the reactive center are key to inhibitor activity.

As mentioned previously, **1** was attractive from a medicinal chemistry point of view due to the high tractability offered by its structure. Scheme 1 shows the synthetic approach used to

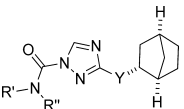
Scheme 1. Overview of Chemistry for Synthesis of **1** and Analogues



prepare the analogues tested. Nucleophilic substitution of aryl bromides **6** by mercaptotriazole **7** with potassium carbonate in DMF yielded the sulfides **8** in good to excellent yields. Reaction of **8** with various carbamoyl chlorides yielded the carbamoyl sulfide analogues of type **9**, which were converted to sulfones **10** in good yield by oxidation with *m*CPBA. Alternatively, the sulfides **8** were oxidized to the triazole sulfones **11** with *m*CPBA in EtOAc. Reaction of **11** with triphosgene in DCM generates a carbamoyl chloride that was reacted in situ with secondary amines to yield analogues of sulfone **10**.

Table 2 shows the results obtained for a series of analogues exploring the steric properties around the carbamoyl group. However, the *N*-Me ¹Pr substitution pattern was found to be optimal (**1**, vide supra). Substitutions with low steric demand such as those in **13–15** exhibited nanomolar levels of in vitro activity. Sterically demanding *N*-substituents such as those in **16–18** were inactive in vitro, most likely due to a decreased reactivity toward the target enzymes. The pyrrolidine analogue **19** showed a similar activity to **1**, while piperidine **21** was less active. The *N*-benzyl compound **22** has a moderate level of activity, **23** and **24**, containing a *N*-phenyl groups had poor activity.

The sulphonyl group is strongly electron withdrawing and as such imparts enhanced leaving group ability onto the triazole. The oxidation level of the sulfur atom, therefore, presents an

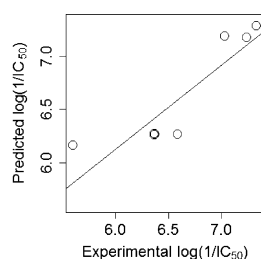
Table 2. In Vitro *Pf* (3D7) IC₅₀s for a Range of Carbamoyl Triazoles^a


-NR'R''	Y	<i>Pf</i> IC ₅₀ (μM) (SD)	-NR'R''	Y	<i>Pf</i> IC ₅₀ (μM) (SD)
	-S-	12 0.071 (± 0.024)		-S-	20 0.178 (± 0.021)
	-SO ₂ -	13 0.047 (± 0.015)		-SO ₂ -	21 0.626 (± 0.114)
	-S-	14 0.141 (± 0.005)		-SO ₂ -	22 0.256 (± 0.075)
	-SO ₂ -	15 0.093 (± 0.006)		-SO ₂ -	23 2.69 (± 0.879)
	-SO ₂ -	16 >5 (NA)		-S-	24 >5 (NA)
	-SO ₂ -	17 >5 (NA)		-SO ₂ -	25 0.585 (± 0.013)
	-S-	18 1.42 (± 0.006)		-S-	26 2.240 (± 0.210)
	-SO ₂ -	19 0.084 (± 0.015)		-SO ₂ -	27 0.145 (± 0.031)

^aAtovaquone was used as positive control with IC₅₀ = 0.001 μM

opportunity to temper the reactivity of the carbamoyl group. A range of sulfide analogues were synthesized and their in vitro activities compared with those of the corresponding sulfones. Although differences in activity were observed, it was not possible to establish any SAR conclusions regarding the preferred oxidation state of the sulfur atom from these results.

Quantum mechanical calculations were performed in order to investigate if differences in antimalarial activity were attributable to the oxidative state of the sulfur atom [(II) and (VI)] (Table 2). Given the proposed mechanism of action of this chemotype, we hypothesized that electronic structure calculations might be able to capture aspects of a compound's reactivity and relate those to measured IC₅₀s. Several descriptors derived from the calculations were investigated including LUMO, electronegativity, and softness (see Supporting Information (SI) for a complete list). A good linear correlation ($r^2 = 0.79$) was found between the "softness" of the molecules and the measured in vitro IC₅₀ values (Figure 5). The model passed tests for validity (see SI) and had a good 5-fold cross validation r^2 value of 0.65 ± 0.07 indicative of a robust model. The softness of a molecule is a measure of a

**Figure 5.** Plot of experimental log(1/IC₅₀) vs predicted log(1/IC₅₀) using calculated molecular softness.

compound's polarizability and electronegativity and is consistent with the proposed antimalarial mechanism of action, i.e., carbonyl reactivity with protein nucleophiles.

The S-substituent was also varied from the original *exo*-norbornane (Table 3). Cyclohexyl substitution provided 28, a

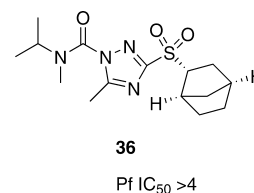
Table 3. In Vitro *Pf* (3D7) IC₅₀s for Carbamoyl Triazoles Containing Different S-Substituents^a

Compound	<i>Pf</i> IC ₅₀ (μM)	Compound	<i>Pf</i> IC ₅₀ (μM)
	28 0.028		32 1.895
	29 0.008		33 0.164
	30 0.571		34 0.418
	31 0.019		35 1.438

^aAtovaquone was used as positive control with IC₅₀ = 0.001 μM

compound endowed with slightly improved potency. The bulky, lipophilic 2-adamantyl group provided the highly potent 29. Aromatic groups attached directly to sulfur 30–33 resulted in lower activity except the highly potent 31. The S-benzyl compounds 34 and 35 were considerably less active than the corresponding norbornyl analogues 19 and 20.

The C-5 of the triazole also offers an opportunity to increase steric demand around the carbamoyl group; however, the S-Me compound 36 proved to be inactive (Figure 6).

**Figure 6.** In vitro *Pf* (3D7) IC₅₀ for 36.

To assist in analyzing and interpreting the SAR associated with the compounds synthesized, QSAR models were developed for the quantitatively measured IC₅₀ values. Initially, models were built using the quantum mechanical approach as described above, however, none of the models explored using a genetic algorithm multiple linear regression approach were satisfactory (data not shown). An alternative nonlinear approach was employed in which models were constructed using random forests³² within a multiple cross-validation scheme³³ to select the optimal parameter (mtry) to use with the molecular descriptors³⁴ (for further computational details, see the SI). We adopted this approach of using multiple training and test sets as every sample may be needed for the

model,³² and previous studies have indicated the inadequacies of using single test set to assess predictive power.³⁵ Indeed, often the performance estimates superior to a single test set because they evaluate many alternate versions of the data.³³ The multiple cross validation approach showed that an mtry value of 109 was optimal with ($r^2 = 0.94 \pm 0.20$). Applying this model gave an excellent overall fit with the antimalarial activity (Figure 7A, $r^2 = 0.92$). The top 10 most influential descriptors

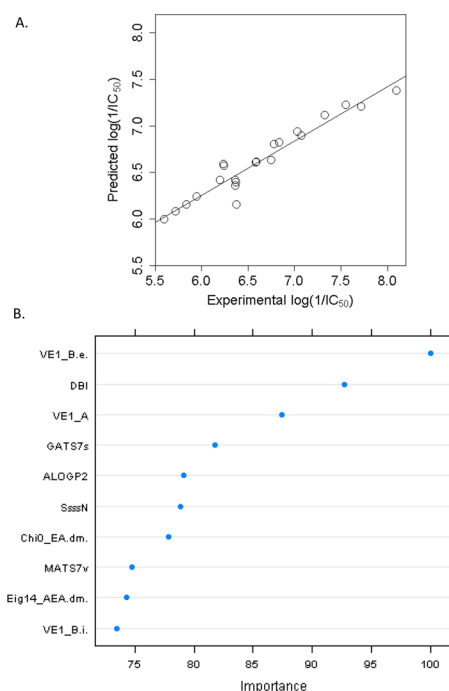


Figure 7. (A) Plot of experimental $\log(1/IC_{50})$ vs predicted $\log(1/IC_{50})$ of the entire quantitative data set. (B) Relative importance of the top 10 most influential descriptors in the model.

are shown in Figure 7B (definitions of descriptors are provided in the SI). Most of these descriptors are challenging to interpret directly, however the utility of the robust QSAR developed would be of value in future virtual screening studies to inform and prioritize synthesis and testing.

Further insight into the behavior of the carbamoyl triazoles comes from observations regarding the 48 vs 72 h IC_{50} values, and the results are shown in Table 4. However, none of the compounds tested showed any significant difference in IC_{50} between the two time points.

Table 4. In vitro Pf IC_{50} at 48 and 72 h for Carbamoyl Triazoles^a

compd	Pf IC_{50} (μ M) (SD)	
	48 h	72 h
1	0.016 (± 0.001)	0.028 (± 0.004)
17	>5 (NA)	>5 (NA)
18	1.428 (± 0.006)	0.537 (± 0.185)
19	0.037 (± 0.002)	0.037 (± 0.002)
22	0.247 (± 0.086)	0.379 (± 0.196)
23	2.686 (± 0.879)	2.713 (± 0.237)

^aAtovaquone was used as positive control with 48/72 h IC_{50} s: 0.001 μ M (48 h)/0.0003 μ M (72 h)

A screen of several, structurally diverse analogues was then undertaken to establish the metabolic stability in both mouse and human liver microsomes (Table 5). The di-isopropyl-

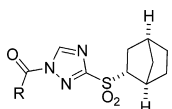
Table 5. In Vitro Clearance and Half Lives in Mouse and Human Liver Microsomes for Carbamoyl Triazoles

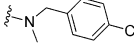
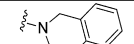
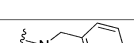

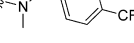
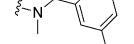
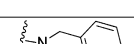
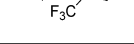
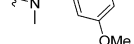
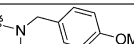
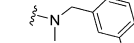
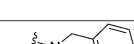
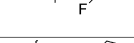


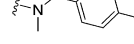
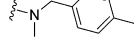
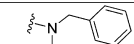

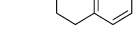
compd	mouse		human	
	in vitro Cl_{int} ($mL \cdot min^{-1} \cdot g^{-1}$)	in vitro $t_{1/2}$ (min)	in vitro Cl_{int} ($mL \cdot min^{-1} \cdot g^{-1}$)	in vitro $t_{1/2}$ (min)
18	22.0	<5	3.1	22.3
19	>30	<5	1.0	>30
20	>30	<5	1.5	>30
22	4.0	19.4	1.5	>30

containing 18 showed an in vitro intrinsic clearance in mouse liver microsomes of $22.0 \text{ mL} \cdot \text{min}^{-1} \cdot \text{g}^{-1}$, very similar to that of 1. The pyrrolidine analogues 19 and 20 both exhibit higher clearance ($>30 \text{ mL} \cdot \text{min}^{-1} \cdot \text{g}^{-1}$) than 1. These values all correspond to in vitro $t_{1/2}$ values of <5 min. This data suggests that high clearance in mouse liver microsomes is a common feature across the series of compounds containing exclusively aliphatic *N*-substituents. However, all of these compounds showed much lower clearance in human liver microsomes. 22 showed an improved clearance in the mouse microsomes of $4.0 \text{ mL} \cdot \text{min}^{-1} \cdot \text{g}^{-1}$ which corresponds to an in vitro $t_{1/2}$ of almost 20 min.

With the improved metabolic stability and reduced clearance exhibited by 22, it was decided to investigate the SAR around the benzyl group with a view to obtaining higher potency. A series of benzyl analogues were synthesized, and the results are shown in Table 6. Addition of a chlorine atom in the 4- (37) or 2- (38) position led to a slight reduction in activity compared to 22, 3-Cl analogue 39 maintained the same activity. Trifluoromethyl substitution (40–42) led to a reduction in activity with 40 and 39 being significantly less active than 22. 3-OMe analogue 43 showed an improvement in potency over 22 and the 4-OMe 44 was extremely potent in the low nanomolar range (10 nM). The 2,4-dimethoxy substituted 45 was also highly potent (30 nM). Fluoro substituted compounds 46–48 showed similar activity to 22 with the position of F-substitution having little effect on the activity. Introduction of a heterocycle such as pyridine in 49 (86 nM) was well tolerated and slightly more potent than 22. While 4-SO₂Me had negligible impact on potency (50), 4-Ac and 4-*t*Bu analogues were both highly active displaying IC_{50} values of 50 and 16 nM, respectively. The 3-CN benzyl substituted 53 and the bicyclic tetrahydroisoquinoline 54 were inactive. It was previously observed that the diisopropyl analogue 17 was significantly more stable in blood compared to 1 (Figure S2), presumably a result of the highly sterically demanding substitution around the carbamoyl group. Because of the potency exerted by the 4-OMe benzyl group and the stabilizing ability of bulky aliphatic groups, 55 and 56 were synthesized containing cyclopropyl and isopropyl groups, respectively. However, the in vitro activities of these compounds were too low to warrant further investigation.

The two most potent compounds, 44 and 52, were then evaluated for microsomal stability. 44 ($Cl_{int} = 3.0 \text{ mL} \cdot \text{min}^{-1} \cdot \text{g}^{-1}$; $t_{1/2} = 22.6 \text{ min}$) showed a similar clearance value to that of 22 (vide supra) in mouse liver microsomes, and 52 had a lower metabolic stability under the same conditions ($Cl_{int} = 7.8 \text{ mL} \cdot \text{min}^{-1} \cdot \text{g}^{-1}$; $t_{1/2} = 9.0 \text{ min}$). The ChromLogD (pH 7.4) for 44 and 52 were 5.72 and 7.69, respectively. 44 was significantly

Table 6. In Vitro IC₅₀s for N-Benzyl Substituted Carbamoyl Triazoles vs the 3D7 Strain of *Plasmodium falciparum*^a


R	Compound	Pf IC ₅₀ (μM) (SD)
	37	0.602 (± 0.084)
	38	0.725 (± 0.162)
	39	0.307 (± 0.089)
	40	0.554 (± 0.008)
	41	1.862 (± 0.368)
	42	1.263 (± 0.157)
	43	0.036 (± 0.004)
	44	0.010 (± 0.002)
	45	0.040 (± 0.011)
	46	0.197 (± 0.079)
	47	0.373 (± 0.015)
	48	0.180 (± 0.029)
	49	0.086 (± 0.013)
	50	0.290 (± 0.065)
	51	0.050 (± 0.015)
	52	0.016 (± 0.01)
	53	3.43 (± 0.511)
	54	>5 (NA)
	55	1.023 (± 0.118)
	56	0.84 (± 0.05)

^aAtovaquone was used as positive control with 48 h IC₅₀: 0.001 μM.

more soluble (CLND) than **52**, where maximum concentrations were measured at 125 and 28 μM, respectively. Cytotoxicity assays against HepG2 cells revealed IC₅₀ > 100 μM for **44** and = 75.2 μM for **52**.

Given the slightly higher potency, reduced in vitro clearance, adequate toxicological profile, and superior physicochemical properties of **44**, an in vivo oral efficacy study was initiated with this compound. The experiment was carried out in the GSK *Pf* humanized mouse model of infection in a standard four-day assay as described by Jiménez-Díaz.³⁶ In this assay, **44** was efficacious against *P. falciparum* in vivo showing an ED₉₀ ≈ 128 mg kg⁻¹ (Figure 8A) and clear phenotypic effects on parasites remaining in blood (Figure 8B) were observed. Interestingly, **44** was not detected in peripheral blood of infected humanized mice. This apparent disconnect between the in vivo efficacy and levels in blood of **44** could be related to the instability of the compound in blood.

To further characterize the profiles of **1** and **44**, we conducted a phenotypic assay to assess the effects of the two compounds on the parasite life cycle (Figure 9). In the presence of **1** and **44**, the parasites could be found as primarily young trophozoites at both 24 and 48 h after drug treatment. Parasites are arrested in young trophozoite stage comparable to atovaquone-treated parasites included as control.

The final part of our study was focused on establishing if this chemotype had the potential to target the best characterized

malarial serine proteases examined to date, PfSUB1 (*Pf* subtilisin like serine protease-1). This enzyme is released into the parasitophorous vacuole where it activates a family of protease-like proteins called SERA, leading to rupture of the vacuole and host cell membrane.^{37–39} Inhibition of PfSUB1 is a promising approach to block propagation of a malarial infection by preventing the egress of merozoites from the red blood cell.³⁹ **1**, **12**, **18**, **34**, and **44** were screened against this target, and none of the azole compounds showed inhibitory activity against this serine protease. The positive control NF2114 compound showed good inhibition, with an IC₅₀ of ~3 μM (SI). This result indicates that the novel molecules prepared here, and the known serine protease inhibitor carbamoyl triazole **1** are likely targeting novel uncharacterized plasmodial serine protease enzymes.

CONCLUSIONS

The carbamoyl triazole series (**1**) belonging to the TCAMS is a promising new compound class for antimalarial agents that potentially work by inhibition of novel serine protease targets other than PfSUB1. Analogue synthesis led to several compounds with low nanomolar in vitro activity. The *N*-benzyl series contains several highly potent compounds with low nanomolar activity such as **44**, **45**, **51**, and **52**. These new molecules display a greatly improved metabolic stability over

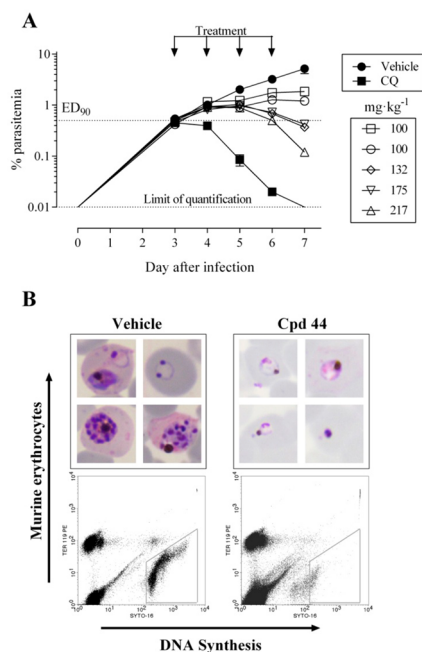


Figure 8. Efficacy of **44** against the human malaria parasite in the GSK *Pf* humanized mouse model. (A) Parasitemia in individual mice treated with different doses of **44** during the efficacy assay. Each open symbol represents an individual mouse treated with **44**. Solid symbols are the average of $n = 4$ mice treated with vehicle (solid circle) and $n = 2$ treated po with chloroquine at 10 mg·kg⁻¹ (solid square). (B) Microscopic and flow cytometry analysis of *P. falciparum* present in peripheral blood of mice treated with vehicle or **44** at 217 mg·kg⁻¹. Samples were taken 96 h after starting the treatment. Flow cytometry dot plots from samples of peripheral blood show *P. falciparum*-infected human erythrocytes (polygonal region). Animals treated with vehicle show healthy nonsynchronized asexual stages, whereas the parasites present in **44**-treated animals are altered rings, abnormal trophozoites with hemozoin granules and pyknotic cells.

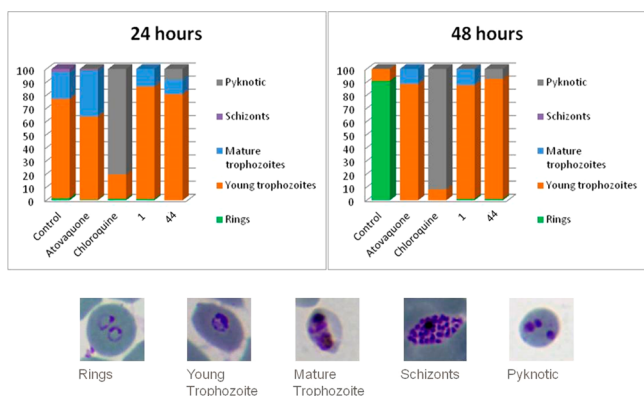


Figure 9. Phenotypic parasite populations examined by microscopy at 0, 24, and 48 h for **1** and **44**. In vitro *P. falciparum* phenotypic profile was determined for **1** and **44** at 10 \times their respective *Pf* IC₅₀, and standard antimalarials were also included as controls: atovaquone and chloroquine.

the hit compound **1** in mouse liver microsomes. **44** is orally efficacious in a SCID mouse model of *Pf* infection with an ED₅₀ and ED₉₀ of approximately 100 and 150 mg kg⁻¹, respectively. The results presented warrant further investigation to identify the target of these highly active compounds.

■ ASSOCIATED CONTENT

§ Supporting Information

The Supporting Information is available free of charge on the ACS Publications website at DOI: 10.1021/acs.jmedchem.5b00434.

Molecular formula strings (XLSX)

General experimental procedures and characterization data for all synthesized compounds (PDF)

■ AUTHOR INFORMATION

Corresponding Authors

*For F.C.: phone, +44 793108881; e-mail, felix.r.calderon-romo@gsk.com.

*For P.M.O.: phone, + 44 151 794 3553; e-mail, pmoneill@liv.ac.uk.

Present Address

¹For F.C.: Immuno-inflammation Therapy Area Unit, GSK, Gunnels Wood Road, Stevenage, Hertfordshire, SG1 2NY, UK.

Notes

The human biological samples were sourced ethically and their research use was in accord with the terms of the informed consents. All animal studies were ethically reviewed and carried out in accordance with European Directive 2010/63/EU and the GSK Policy on the Care, Welfare and Treatment of Animals.

The authors declare no competing financial interest.

■ ACKNOWLEDGMENTS

We gratefully acknowledge the Tres Cantos OpenLab Foundation for funding (project TC042), registered as a limited company no. 7301222, registered as a charity in England and Wales no. 1142577. We also thank Dr. Bárbara Villa Marcos for assistance with proofreading the manuscript and Dr. Tony Mete for helpful discussions around protease inhibitor drug design.

■ REFERENCES

- (1) *World Malaria Report 2013*; WHO: Geneva, 2013; pp 1–255.
- (2) Schlitzer, M. Antimalarial drugs - What is in use and what is in the pipeline. *Arch. Pharm.* **2008**, *341*, 149–163.
- (3) Berman, J. Toxicity of commonly-used antimalarial drugs. *Travel Med. Infect. Dis.* **2004**, *2*, 171–84.
- (4) Cravo, P.; Culleton, R.; Afonso, A.; Ferreira, I. D.; do Rosario, V. E. Mechanisms of drug resistance in malaria: Current and new challenges. *Anti-Infect. Agents Med. Chem.* **2006**, *5*, 63–73.
- (5) Farooq, U.; Mahajan, R. C. Drug resistance in malaria. *J. Vector Borne Dis.* **2004**, *41*, 45–53.
- (6) White, N. J. Antimalarial drug resistance. *J. Clin. Invest.* **2004**, *113*, 1084–1092.
- (7) Winstanley, P. A.; Ward, S. A.; Snow, R. W. Clinical status and implications of antimalarial drug resistance. *Microbes Infect.* **2002**, *4*, 157–164.
- (8) Wongsrichanalai, C.; Pickard, A. L.; Wernsdorfer, W. H.; Meshnick, S. R. Epidemiology of drug-resistant malaria. *Lancet Infect. Dis.* **2002**, *2*, 209–218.
- (9) Kyaw, M. P.; Nyunt, M. H.; Chit, K.; Aye, M. M.; Aye, K. H.; Lindegardh, N.; Tarning, J.; Imwong, M.; Jacob, C. G.; Rasmussen, C.; Perin, J.; Ringwald, P.; Nyunt, M. M. Reduced Susceptibility of *Plasmodium falciparum* to Artesunate in Southern Myanmar. *PLoS One* **2013**, *8*, e57689.
- (10) Noedl, H.; Se, Y.; Schaefer, K.; Smith, B. L.; Socheat, D.; Fukuda, M. M. Evidence of Artemisinin-Resistant Malaria in Western Cambodia. *N. Engl. J. Med.* **2008**, *359*, 2619–2620.

- (11) Wongsrichanalai, C.; Sibley, C. H. Fighting drug-resistant *Plasmodium falciparum*: the challenge of artemisinin resistance. *Clin. Microbiol. Infect.* **2013**, *19*, 908–916.
- (12) Dondorp, A. M.; Nosten, F.; Yi, P.; Das, D.; Phyto, A. P.; Tarning, J.; Lwin, K. M.; Arie, F.; Hanpithakpong, W.; Lee, S. J.; Ringwald, P.; Silamut, K.; Imwong, M.; Chotivanich, K.; Lim, P.; Herdman, T.; An, S. S.; Yeung, S.; Singhasivanon, P.; Day, N. P. J.; Lindegardh, N.; Socheat, D.; White, N. J. Artemisinin Resistance in *Plasmodium falciparum* Malaria. *N. Engl. J. Med.* **2009**, *361*, 455–467.
- (13) Burrows, J. N.; Hooft van Huijsduijnen, R.; Möhrle, J. J.; Oeuvray, C.; Wells, T. N. C. Designing the next generation of medicines for malaria control and eradication. *Malar. J.* **2013**, *12*, 187.
- (14) Gamo, F.-J.; Sanz, L. M.; Vidal, J.; de Cozar, C.; Alvarez, E.; Lavandera, J.-L.; Vanderwall, D. E.; Green, D. V. S.; Kumar, V.; Hasan, S.; Brown, J. R.; Peishoff, C. E.; Cardon, L. R.; Garcia-Bustos, J. F. Thousands of chemical starting points for antimalarial lead identification. *Nature* **2010**, *465*, 305–U56.
- (15) Calderon, F.; Barros, D.; Bueno, J. M.; Coteron, J. M.; Fernandez, E.; Gamo, F. J.; Lavandera, J. L.; Leon, M. L.; MacDonald, S. J. F.; Mallo, A.; Manzano, P.; Porras, E.; Fiandor, J. M.; Castro, J. An Invitation to Open Innovation in Malaria Drug Discovery: 47 Quality Starting Points from the TCAMS. *ACS Med. Chem. Lett.* **2011**, *2*, 741–746.
- (16) Baumann, E.; Zagar, C.; Kardorff, U.; Misslitz, U.; Westphalen, K.-O.; Walter, H.; Hamprecht, G. Substituted carbamoyl triazoles and their use as herbicides. CA 2264708 A1, 1997.
- (17) Iwabuchi, H.; Konosu, T.; Mori, M.; Uchida, T.; Watanabe, T. Carbamoyl-bearing triazole fungicides. WO 2002040472 A1, 2002.
- (18) Watkins, T. I.; Weighton, D. M. Triazole insecticides. US 4054664 A, 1974.
- (19) Akahoshi, F.; Takeda, S.; Okada, T.; Kajii, M.; Nishimura, H.; Sugiura, M.; Inoue, Y.; Fukaya, C.; Naito, Y.; Imagawa, T.; Nakamura, N. Synthesis and pharmacological activity of triazolo 1,5-a triazine derivatives inhibiting eosinophilia. *J. Med. Chem.* **1998**, *41*, 2985–2993.
- (20) Ebdrup, S.; Sørensen, L. G.; Olsen, O. H.; Jacobsen, P. Synthesis and structure-activity relationship for a novel class of potent and selective carbamoyl-triazole based inhibitors of hormone sensitive lipase. *J. Med. Chem.* **2004**, *47*, 400–410.
- (21) Adibekian, A.; Martin, B. R.; Wang, C.; Hsu, K.-L.; Bachovchin, D. A.; Niessen, S.; Hoover, H.; Cravatt, B. F. Click-generated triazole ureas as ultrapotent in vivo-active serine hydrolase inhibitors. *Nat. Chem. Biol.* **2011**, *7*, 469–478.
- (22) Yasuda, N.; Nagakura, T.; Yamazaki, K.; Yoshikawa, S.; Okada, T.; Ikuta, H.; Koyanagi, M. Pharmaceutical use of *N*-carbamoylazole derivatives. US7238720 B2, 2007.
- (23) Alam, A. Serine Proteases of Malaria Parasite *Plasmodium falciparum*: Potential as Antimalarial Drug Targets. *Interdiscip. Perspect. Infect. Dis.* **2014**, *2014*, 453186–453186.
- (24) Breton, C. B. Plasmodium serine proteases implicated in red blood cell invasion: Molecular characterization and validation as drug targets. *Biosci. Rep.* **2003**, *23*, 22.
- (25) Howell, S. A.; Well, I.; Fleck, S. L.; Kettleborough, C.; Collins, C. R.; Blackman, M. J. A single malaria merozoite serine protease mediates shedding of multiple surface proteins by juxtamembrane cleavage. *J. Biol. Chem.* **2003**, *278*, 23890–23898.
- (26) Koussis, K.; Withers-Martinez, C.; Yeoh, S.; Child, M.; Hackett, F.; Knuepfer, E.; Juliano, L.; Woehlbier, U.; Bujard, H.; Blackman, M. J. A multifunctional serine protease primes the malaria parasite for red blood cell invasion. *EMBO J.* **2009**, *28*, 725–735.
- (27) Suarez, C.; Volkmann, K.; Gomes, A. R.; Billker, O.; Blackman, M. J. The Malarial Serine Protease SUB1 Plays an Essential Role in Parasite Liver Stage Development. *PLoS Pathog.* **2013**, *9*, e1003811.
- (28) Yeoh, S.; Hackett, F.; Fleck, S. L.; Blackman, M. J. Structure-function analysis of PfSUB-2, a serine protease of the *Plasmodium falciparum* merozoite. *Exp. Parasitol.* **2003**, *105*, 75.
- (29) Young, R.; Green, D. V. S.; Luscombe, C. N.; Hill, A. P. Getting Physical in Drug Discovery II: the Impact of Chromatographic Hydrophobicity Measurements and Aromaticity. *Drug Discovery Today* **2011**, *16*, 822–830.
- (30) Hansen, L.; Deacon, C. F.; Ørskov, C.; Holst, J. J. Glucagon-like peptide-1-(7–36)amide is transformed to glucagon-like peptide-1-(9–36)amide by dipeptidyl peptidase IV in the capillaries supplying the L cells of the porcine intestine. *Endocrinology* **1999**, *140*, S356–S363.
- (31) Sanz, L. M.; Crespo, B.; De-Cozar, C.; Ding, X. C.; Llergo, J. L.; Burrows, J. N.; Garcia-Bustos, J. F.; Gamo, F.-J. *P. falciparum* In vitro Killing Rates Allow to Discriminate between Different Antimalarial Mode-of-Action. *PLoS One* **2012**, *7*, e30949.
- (32) Svetnik, V.; Liaw, A.; Tong, C.; Culberson, J. C.; Sheridan, R. P.; Feuston, B. P. Random forest: a classification and regression tool for compound classification and QSAR modeling. *J. Chem. Inf. Model.* **2003**, *43*, 1947–1958.
- (33) *Applied Predictive Modeling*; Kuhn, M., Johnson, K., Eds.; Springer: New York, DOI 10.1007/978-1-4614-6849-3, pp 61–92.
- (34) *Dragon, Software for Molecular Descriptor Calculation*, Version 6.0; Talete srl: Milano, Italy, 2014; <http://www.talete.mi.it/>.
- (35) Hawkins, D.; Basak, S.; Mills, D. (2003). “Assessing Model Fit by Cross-Validation.” *J. Chem. Inf. Model.* **2003**, *43*, 579–586.
- (36) Jimenez-Diaz, M. B.; Mulet, T.; Viera, S.; Gomez, V.; Garuti, H.; Ibanez, J.; Alvarez-Doval, A.; Shultz, L. D.; Martinez, A.; Gargallo-Viola, D.; Angulo-Barturen, I. Improved Murine Model of Malaria Using *Plasmodium falciparum* Competent Strains and Non-Myelodepleted NOD-scid IL2R gamma(null) Mice Engrafted with Human Erythrocytes. *Antimicrob. Agents Chemother.* **2009**, *53*, 4533–4536.
- (37) Koussis, K.; Withers-Martinez, C.; Yeoh, S.; Child, M.; Hackett, F.; Knuepfer, E.; Juliano, L.; Woehlbier, U.; Bujard, H.; Blackman, M. J. (2009) A multifunctional serine protease primes the malaria parasite for red blood cell invasion. *EMBO J.* **2009**, *28*, 725–735.
- (38) Ruecker, A.; Shea, M.; Hackett, F.; Suarez, C.; Hirst, E. M.; Milutinovic, K.; Withers-Martinez, C.; Blackman, M. J. (2012) Proteolytic activation of the essential parasitophorous vacuole cysteine protease SERA6 accompanies malaria parasite egress from its host erythrocyte. *J. Biol. Chem.* **2012**, *287*, 37949–37963.
- (39) Yeoh, S.; O'Donnell, R. A.; Koussis, K.; Dluzewski, A. R.; Ansell, K. H.; Osborne, S. A.; Hackett, F.; Withers-Martinez, C.; Mitchell, G. H.; Bannister, L. H.; Bryans, J. S.; Kettleborough, C. A.; Blackman, M. J. Subcellular discharge of a serine protease mediates release of invasive malaria parasites from host erythrocytes. *Cell* **2007**, *131*, 1072–1083.